JMEPEG (2011) 20:1364–1369
DOI: 10.1007/s11665-011-9944-x

1059-9495/$19.00

Effect of Cold-rolling on Mechanical Properties and Microstructure of an Al-12%Si-0.2%Mg Alloy

Hengcheng Liao, Mingdong Cai, Qiumin Jing, and Ke Ding

(Submitted November 7, 2010; in revised form January 30, 2011)

Effect of multi-pass cold-rolling on the mechanical properties and microstructure of a near-eutectic Al-12%Si-0.2%Mg casting alloy was investigated. Optical microscopy, SEM, and TEM were employed to resolve the as-rolled microstructure, and the microstructure of samples after aging treatment. It has been found that Brinell hardness increases considerably with rolling reduction ratio; and further annealing leads to a remarkable drop in hardness. Two mechanisms, namely precipitation hardening and recovery softening, were found to develop simultaneously in the subsequent aging treatment following cold rolling. In contrast, recovery softening dominated the aging of cold-rolled specimen with prior intermediate annealing. Tensile properties were also performed to measure the effect of cold rolling and subsequent aging treatment.

Keywords aging, Al-Si alloy, cold rolling, dynamic precipitation

1. Introduction

Study on thermo-mechanical treatment of aluminum alloy can date back to the 1960s. Intermediate thermo-mechanical treatment in aluminum alloy has been reported to be effective in refining as-cast microstructure, eliminating casting defects and increasing fracture toughness. Among those practices, cold rolling has been applied in a large variety of aluminum alloys to acquire optimized microstructure and to meet the desired mechanical and physical properties, such as 2xxx series (Ref 1-4), 3xxx series (Ref 5-7), 5xxx series (Ref 8-10), 6xxx series (Ref 11), and 7xxx series (Ref 1, 12).

Panagopoulos and Georgiou (Ref 9) reported that cold rolling of 5083 led to a significant increase of the surface micro-hardness and a decrease of friction coefficient. Nah et al. (Ref 13) discussed the effect of strain states during cold rolling on the recrystallized grain size. Further, the deformation texture development in AA5182 during cold rolling has been investigated by Chowdhury (Ref 8). It has also been reported that cold rolling direction has an important influence on recrystallization and the evolution of recrystallization texture of continuous cast AA3105 (Ref 6). Cold deformation not only has an important influence on the microstructure evolution, but also impacts subsequent aging response. Traditional heat-treatment procedure of a precipitation-hardened alloy comprises an initial solution treatment, quench (usually to room temperature), and a final aging treatment. It is well known that the reactions associated with aging treatment (i.e., nucleation, growth, and coarsening) can be strongly influenced by prior plastic deformation. Ning et al. (Ref 1) found accelerated aging responses occurred in 2024 and 7A04 aluminum alloys when treated with cold deformation after solution treatment. Similar behavior has also been confirmed in 2014 (Ref 2, 4), AA3003 (Ref 5), and Al-12wt.%Mg alloys (Ref 14). It has been well accepted that high density of dislocations and micro-segregation of the solute atoms at the dislocation network play key roles in the subsequent aging reaction.

Al-Si-Mg alloys are the most widely used commercial aluminum casting alloys due to the facts that high content of Si lowers the cost, improves the castability, and maintains high specific strength, good corrosion resistance, and weldability (Ref 15-21). However, a great amount of eutectic Si particles present in the microstructure of Al-Si-Mg alloys would be expected to make microstructural evolution complex during cold deformation; and impact subsequent heat treatments. Recently, near-eutectic Al-Mg-Si alloy has been paid more attention. In our study, cold rolling was applied after solution treatment on Al-12wt.%Si-0.2%Mg alloy to further improve the strength.

2. Experimental Procedure

The base alloy was prepared by melting Al-12.3wt.%Si master alloy and magnesium ingot (commercial purity, 99.8% Mg) in an electrical resistance furnace after degassing with C_2Cl_6 and argon. The melt was then held at 720 °C for 30 min before casting into a plate steel mold with a cavity size of $10 \times 150 \times 280$ mm. The chemical composition (weight percentage) of solidified plate was quantified by ARL-4300 as Si 11.96%, Mg 0.20%, Fe 0.17%, Sr 0.02% with balanced Al.

The casting plate was cut into specimens with dimension of $10 \times 30 \times 100$ mm. The specimens were solution-treated at 535 ± 2 °C for 6 h and then quenched into water of room temperature. The solutionized specimens were then cold-rolled at room temperature to different thicknesses. Specimens with

Hengcheng Liao, Mingdong Cai, Qiumin Jing, and **Ke Ding**, Jiangsu Key Laboratory for Advanced Metallic Materials, School of Materials Science and Engineering, Southeast University, Nanjing 211189, China; and **Mingdong Cai**, Wyman-Gordon Forgings, Inc, P.O. Box 40456, Houston, TX 77240. Contact e-mail: hengchengliao@seu.edu.cn.

various thermo-mechanical processing techniques are labeled from A through D with O representing as-cast specimen, details are tabulated in Table 1. It was noted from experiment that cracking was observed on the specimen with a total 40% reduction ratio, thus some specimens cold-rolled to a total 35% reduction ratio underwent an intermediate annealing treatment at 300 °C for 2 h, and then further cold-rolled to a total reduction ratio of 50% by another two passes. Specimens with 20 and 50% total reduction ratios (i.e., Specimen A and D) were then aged at 160 °C for various lengths of time. The intermediate annealing and aging treatment were performed in a furnace with hot-air circulation system and the temperature fluctuation was within 1 °C.

Table 1 Summary of specimen condition

Specimen	Thermo-mechanical processing treatments
O	As-cast
A	Cold-rolled at room temperature to a total 20% reduction ratio by two passes
B	Cold-rolled at room temperature to a total 35% reduction ratio by four passes
C	Cold-rolled at room temperature to a total 35% reduction ratio by four passes; and then underwent an intermediate annealing treatment at 300 °C for 2 h
D	Cold-rolled at room temperature to 35% reduction ratio by four passes; underwent an intermediate annealing treatment at 300 °C for 2 h; and then further cold-rolled at room temperature to a total 50% reduction ratio by two passes

Brinell hardness was measured using a Brinell Rockwell & Vickers optical hardness tester (HBRVU-187.5) and five readings were recorded for each sample. Tensile samples were prepared in accordance with GB/T228-2002 and the testing was carried out on a universal testing machine (CMT4503). The tensile strength and elongation were reported on an average of at least three tests. Optical Microscope (OLYMPUS BX-60M), and JEM-2000EX transmission electron microscope (TEM) with selected area diffraction (SAD) were used to distinguish the microstructure.

3. Results and Discussion

3.1 As-Rolled Microstructure

Figures 1 and 2 shows microstructures deformed by multi-cold-rolling of Al-12%Si-0.2%Mg alloy. It can be seen from Fig. 1(a) that the as-cast dendrite retains almost undeformed for Specimen A; however, with the increase of reduction ratio, the dendrites are seriously deformed and broken dendrites aligned along the rolling direction (Fig. 1b-c). The cracking of eutectic Si particles (light-gray) and Fe-rich intermetallic phases (dark-gray) were observed for all three cases, as shown in Fig. 2. Previously, Umezawa and Nagai (Ref 22) reported that cold deformation imposed on Al-12.6%Si alloy could lead to the secondary phases cracking, after annealing softening, further rolling will force matrix Al to flow into the cracks. In our study, it can be seen from Fig. 2(c) that there is more severe cracking occurred in eutectic Si- and Fe-rich phases (as arrowed). These cracks will act as crack initiation sites when the alloy undergoes further plastic deformation and thus such microstructural

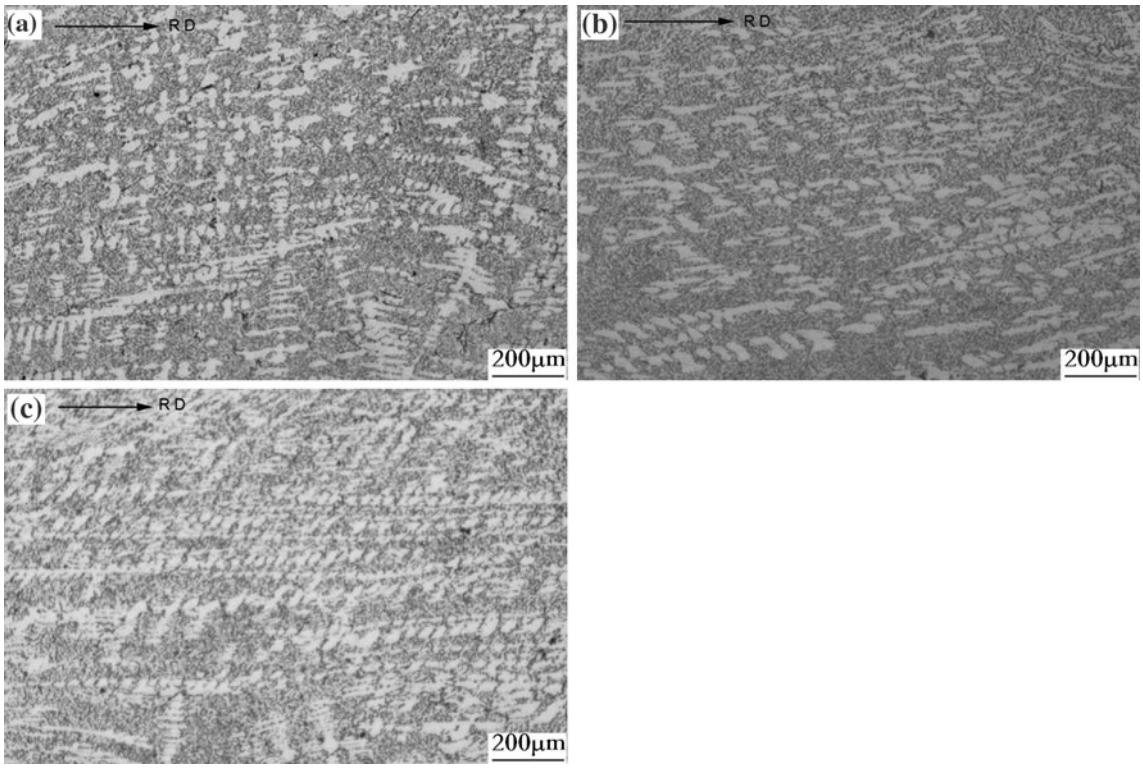

Fig. 1 Optical microstructure of Al-12%Si-0.2%Mg after different rolling passes showing traces of deformation in longitudinal section along rolling direction: (a) Specimen A, (b) Specimen B, and (c) Specimen D

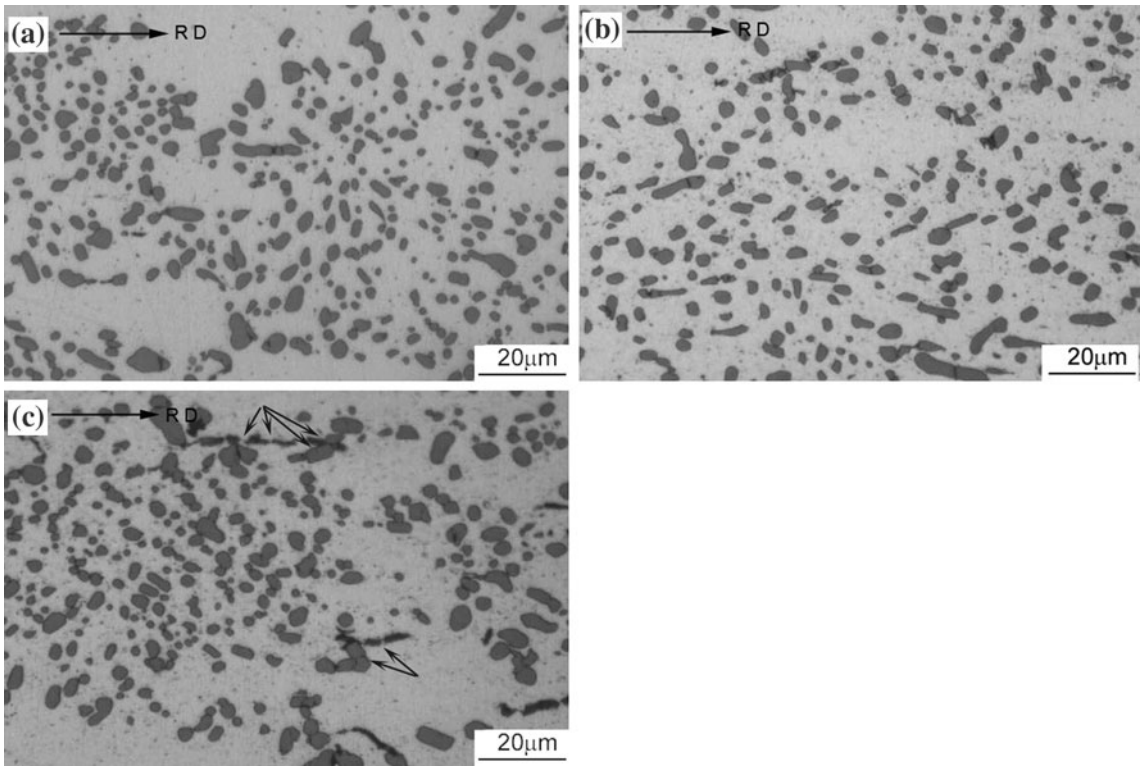

Fig. 2 Optical microstructure of Al-12%Si-0.2%Mg showing cracking of eutectic Si particles (light-gray) and Fe-rich phases (dark-gray) in longitudinal section along rolling direction: (a) Specimen A; (b) Specimen B; and (c) Specimen D

features are detrimental to strength and toughness. A considerable strain hardening is also anticipated due to severe plastic deformation of the matrix (primary dendritic and eutectic Al phase) induced during cold rolling.

3.2 Aging Response

As-rolled hardness with various reduction ratios is summarized in Fig. 3, which shows approximately linear increase in hardness with the reduction ratio up to 35%. Strong strain hardening during cold rolling was observed, i.e., an over 70% increase in hardness when comparing Specimen B (102.2HBS) with as-solution-treated sample (59.1HBS). As expected, the intermediate annealing (2 h at 300 °C) remarkably softened the specimen—hardness dropped from 102.2HBS (Specimen B) to 55.4HBS (Specimen C), as indicated by the dashed line in Fig. 3. Further cold-rolling after the intermediate annealing treatment demonstrates a similar hardening effect as those samples being rolled up to a 35% reduction ratio. Figure 4 shows aging response of two specimens—Specimen A (square) and Specimen D (circle). An obvious precipitate hardening effect is observed for Specimen A, with a peak hardness of 103.5HBS obtained after about 3 h aging at 160 °C—less than half of the peak hardness time required for solutionized sample without prior deformation (i.e., about 8 h). Hardness drop during prolonged aging due to over-aging is also observed. In contrast, a continuous hardness drop during aging has been observed for Specimen D. As a reference, the Brinell hardness of as-cast specimen was about 62.5HBS. After 6 h solution treatment at 535 °C, the hardness dropped to 59.1HBS, and a peak hardness of 70.7HBS was obtained by aging at 160 °C for 8 h.

It is believed that prior plastic deformation invariably accelerates the rate of precipitation by introducing prolific

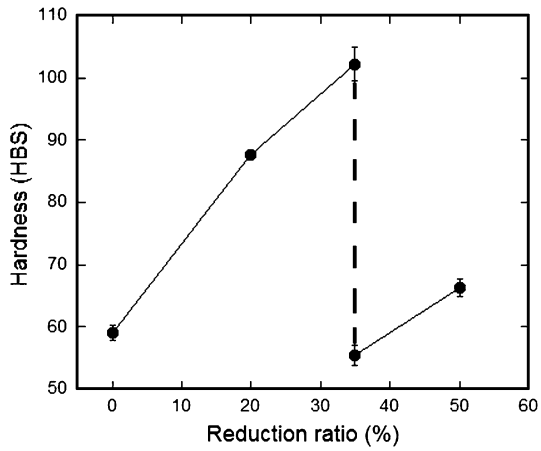

Fig. 3 Hardness versus reduction ratio during a multi-pass cold-rolling process (the dashed line indicates the hardness change after an intermediate annealing)

heterogeneous nucleation sites from supersaturated solid solution. Due to cold deformation, a great amount of dislocation defects is produced (see also Fig. 7), which increases the nucleation site density of precipitation phases. Dislocations also provide quick channels for atom diffusion, thus it accelerates the formation of GP zones during succeeding aging (Ref 5, 23). In addition, cold deformation can cause the redistribution of the precipitate-forming elements between the dislocation cell walls and the cell interiors and hence have a significant effect on the nucleation kinetics of the precipitation (Ref 5). In our study, cold deformation leads to an early aging peak time compared with the specimen without cold deformation. In other words,

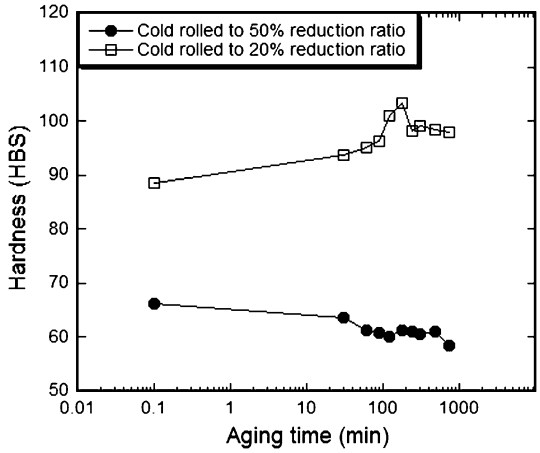

Fig. 4 Hardness variation during an aging treatment at 160 °C: (a) Specimen A and (b) Specimen D

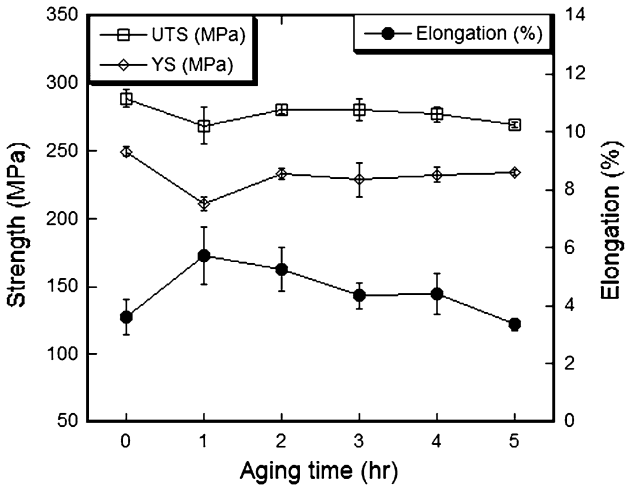

Fig. 5 Tensile properties variation as a function of aging time in Specimen A

it accelerates the aging response, which is consistent with the previous findings (Ref 1, 2, 4, 5, 14). However, no precipitation hardening occurred in aging Specimen D, and conversely the monotonic drop in hardness with aging time indicates a temperature-dependent recovery softening effect.

3.3 Mechanical Properties

The phenomena of aging-hardening (in Specimen A) or recovery-softening (in Specimen D) are more clearly demonstrated from tensile properties, as shown in Fig. 5 and 6, respectively. For Specimen A, there is an obvious ultimate tensile strength (UTS) drop after being aged for 1 h, which is mainly due to the recovery and stress relaxation. Continuous aging demonstrates a typical aging hardening effect to a peak UTS after 2-3 h and then followed by over aging, during which the UTS decreases with aging time. Correspondingly, the elongation increases initially and then decreases. This indicates that the recovery softening dominates the beginning stage of aging treatment, leading to a considerable reduction in strength and increase in elongation. More rapidly in the following aging treatment, precipitation hardening of β-Mg_2Si phase from super

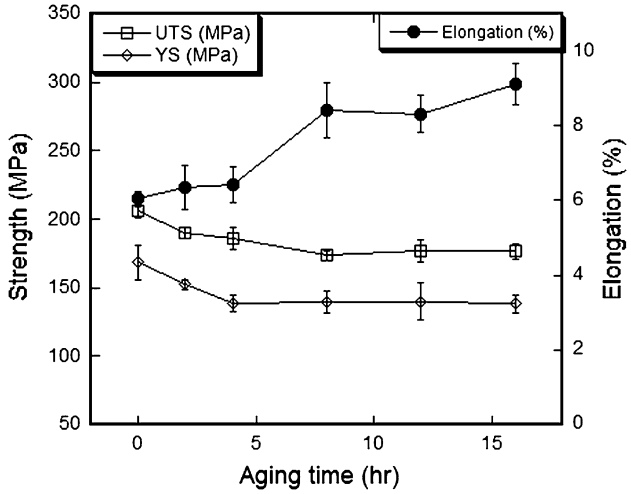

Fig. 6 Tensile properties variation as a function of aging time in Specimen D

saturation solution exerts its impact on mechanical properties, and one can see the strength begins to increase and then decreases after peak strength was reached, exhibiting a typical aging hardening behavior. Though it is noted that the as-rolled specimen possess the highest yield strength and UTS, the unstable structure (featured with high volume of subgrains and high dislocation density) accompanying with poor ductility makes the subsequent aging treatment a must.

But for Specimen D, the strength and elongation monotonically decreases and increases with aging time, respectively (Fig. 6). This indicates there is no or weak precipitation hardening effect during subsequent aging, instead, recovery-softening dominates this process. Such finding is in contradiction to the study reported in alloy 6082 (Ref 24). It is believed that precipitation occurring in the intermediate annealing process plays a critical role in influencing materials mechanical properties during subsequent cold rolling and aging treatment. In other words, dislocation-assisted aging has already taken place during the intermediate annealing, which consumed saturated Mg and Si atoms to form β-Mg_2Si. The fact that peak hardness has been reached after aging 3 h at 160 °C following 20% cold rolling (refer to Fig. 4) indicates possible over-aging was already reached during the intermediate annealing (i.e., 2 h at 300 °C) following 35% rolling. No further aging (either dynamic or static) occurs during successive cold rolling (i.e., further 20% reduction ratio) and aging treatment.

3.4 TEM Studies

TEM was carried out to study the effect of intermediate annealing on microstructure in the samples after specimen been cold rolled. Elongated grain structures along the rolling direction and high density dislocations (shown in Fig. 7a) were observed in the specimens right after multi-cold-rolling of a total 35% reduction ratio. The appearance of subgrain/cell structures and some fine precipitates also indicate partial recovery occurred during the severe deformation. Previously, Ferry and Munroe (Ref 25) investigated the microstructural development during cold rolling and static recovery of an Al alloy (AA 2014) and an AA 2014 matrix composite reinforced by 20%Al_2O_3 particles of 15 μm diameter, and found that the addition of the ceramic reinforcement affected the matrix

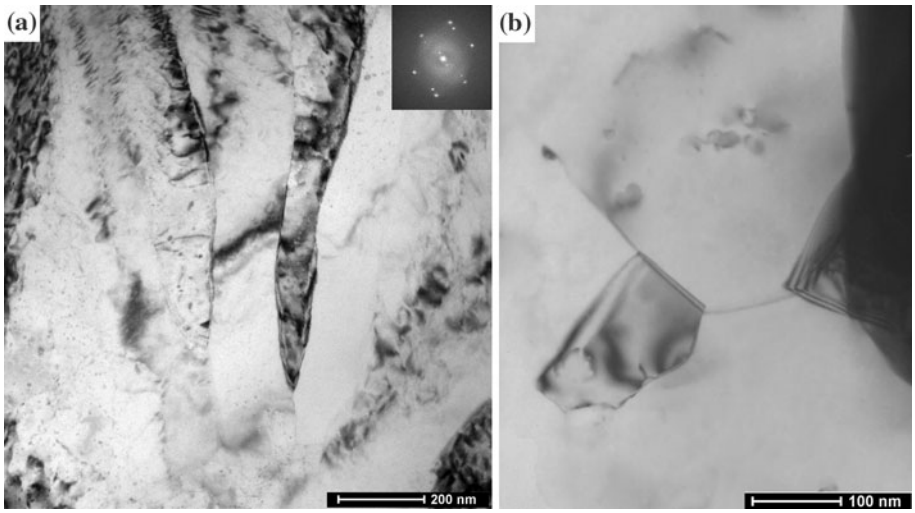

Fig. 7 TEM showing (a) the deformed microstructure in Specimens B (beam direction is near [011]); and (b) recrystallized grain structure in Specimen C

deformation microstructure by refining the cellular substructure near Al_2O_3 particles and generating shear bands and complex deformation zones in the vicinity of particle clusters. Subsequent annealing at 200 °C resulted in a more rapid recovery rate in the composite than the alloy, which was attributable to a larger driving force brought about by the finer cell size near the particles. Liu et al. (Ref 7) did a similar research and proposed that deformation incompatibilities occurred at matrix/particle interfaces lead to the formation of deformation zones around the particles and large lattice rotations. Dynamic recovery was also observed in cold rolled Al-12wt.%Mg alloy (Ref 14). In our study, cold rolling of Al-12wt.%Si-0.2%Mg alloy leads to more severe plastic deformation in the vicinity of the non-deformable eutectic Si particles, which accelerates the following recovery. This evolution of matrix structure is expected to lead to strain strengthening and acceleration of precipitation transformation, so the hardness increases with the reduction ratio (as shown in Fig. 3) and the peak time is advanced considerably for the specimen with cold deformation during successive aging compared with one without cold deformation. A careful examination of Fig. 7(a) also reveals that some fine precipitates formed during cold rolling and uniformly distributed within the elongated grain/subgrain structures. Though one can argue that the fine precipitates could be broken primary or eutectic Si particles during rolling, the shortage of coarse particles in the nearby regions (Fig. 7a) and the relatively uniform size and spatial distribution make it more convincing that those precipitates are β-Mg_2Si phases. Such dynamic precipitation of fine β-Mg_2Si phases from warm or cold deformation has also been previously reported in equal channel angular extrusion process (ECAE) (Ref 26, 27). Further particle identification work using XRD and SEM-EDS techniques is in process.

Typical recrystallized grain structure was observed in Specimen C with intermediate annealing following cold-rolling (Fig. 7b), which indicates that strain strengthening effect has gone almost completely. This microstructural change is also reflected in the abrupt hardness decrease, as shown with the dashed line in Fig. 3. Furthermore, one can see that precipitate coarsening occurred in the intermediate annealing process (comparing Fig. 7a and b). The shortage of excessive solid solution of Mg and Si in the cold-rolled and annealed sample makes subsequent strengthening through cold deformation and aging treatment less effective. Thus, recovery softening effect occurs in the aging treatment of the sample subject to a further cold rolling. Such microstructural evolution in specimen D correlates well with the mechanical property variation, as indicated in Fig. 4 and 5.

4. Conclusions

We studied the effect of various thermal mechanical processing routes on the mechanical properties in an Al-12wt.%Si-0.2%Mg alloy after solutionization, using a combination of multi-pass cold rolling, intermediate annealing, and aging treatment. It has been found that cold rolling leads to considerable strain strengthening, which increases approximately linearly with reduction ratio. Cold deformation introduces a high density of dislocations and more severe plastic deformation in the vicinity of the non-deformable eutectic Si particles, which accelerate the succeeding aging response and the formation of recovery microstructure.

Two mechanisms, namely precipitation hardening and recovery softening, were found to operate simultaneously in the subsequent annealing/aging treatment. Soon after the recovery softening dominates the beginning of aging of cold-rolled materials, precipitation hardening of β-Mg_2Si phase from super saturation solution exerts its influence on mechanical properties. However, for the cold-rolled specimens with the intermediate annealing, recovery softening governs the overall aging course, due to dynamic precipitation of Mg_2Si phase in the prior rolling and precipitate coarsening occurred in the intermediate annealing.

Acknowledgment

The authors would like to thank Prof. Ye Pan and Mr. Aiqun Xu of Southeast University for valuable discussions.

References

1. A.L. Ning, Z.Y. Liu, and S.M. Zeng, Effect of Large Cold Deformation After Solution Treatment on Precipitation Characteristic, Deformation Strengthening of 2024 and 7A04 Aluminum Alloys, *Trans. Nonferrous Met. Soc. China*, 2006, **16**, p 1341–1347
2. S. Sinh and D.B. Goel, Influence of Thermomechanical Aging on Tensile Properties of 2014 Aluminum Alloy, *J. Mater. Sci.*, 1990, **25**, p 3894–3900
3. J.H. Wang, D.Q. Yi, X.P. Su, and F.C. Yin, Influence of Deformation Aging Treatment on Microstructure and Properties of Aluminum Alloy 2618, *Mater. Charact.*, 2008, **59**, p 965–968
4. G. Zhao, H.X. Li, C.M. Liu, and Y.P. Guo, Thermomechanical Aging of 2014 Aluminum Alloy, *J. Northeastern Univ. (Nat. Sci. Ed.)*, 2001, **22**, p 664–667
5. S.P. Chen, N.C. Kuijpers, and S. Zwaag, Effect of Microsegregation and Dislocations on the Nucleation Kinetics of Precipitation in Aluminium Alloy AA3003, *Mater. Sci. Eng. A*, 2003, **341**, p 296–306
6. X.Y. Kong, W.C. Liu, J. Li, and H. Yuan, Deformation and Recrystallization Textures in Straight-Rolled and Pseudo Cross-Rolled AA 3105 Aluminum Alloy, *J. Alloys Compd.*, 2010, **491**, p 301–307
7. Q. Liu, Z.Y. Yao, A. Godfrey, and W. Liu, Effect of Particles on Microstructural Evolution During Cold Rolling of the Aluminum Alloy AA3104, *J. Alloys Compd.*, 2009, **482**, p 264–271
8. S.G. Chowdhury, Development of Texture During Cold Rolling in AA5182 Alloy, *Scripta Mater.*, 2005, **52**, p 99–105
9. C.N. Panagopoulos and E.P. Georgiou, Cold Rolling and Lubricated Wear of 5083 Aluminium Alloy, *Mater. Des.*, 2010, **31**, p 1050–1055
10. S. Sezek and B. Aksakal, Deformation and Temperature Behaviour During Cold, Warm and Hot Flat Rolling of AA5454-O Alloy, *Mater. Des.*, 2009, **30**, p 3450–3459
11. S.K. Panigrahi and R. Jayaganthan, Effect of Rolling Temperature on Microstructure and Mechanical Properties of 6063 Al Alloy, *Mater. Sci. Eng. A*, 2008, **492**, p 300–305
12. D. Wang, Z.Y. Ma, and Z.M. Gao, Effects of Severe Cold Rolling on Tensile Properties and Stress Corrosion Cracking of 7050 Aluminum Alloy, *Mater. Chem. Phys.*, 2009, **117**, p 228–233
13. J.J. Nah, H.G. Kang, M.Y. Huh, and O. Engler, Effect of Strain States During Cold Rolling on the Recrystallized Grain Size in an Aluminum Alloy, *Scripta Mater.*, 2008, **58**, p 500–503
14. D. Hamana, M. Bouchear, and A. Derafa, Effect of Plastic Deformation on the Formation and Dissolution of Transition Phases in Al-12 wt.% Mg Alloy, *Mater. Chem. Phys.*, 1998, **57**, p 99–110
15. Y.N. Kwon, Y.S. Lee, and J.H. Lee, Deformation Behavior of Al–Mg–Si Alloy at the Elevated Temperature, *J. Mater. Process. Technol.*, 2007, **187–188**, p 533–536
16. C.D. Lee, Effects of Microporosity on Tensile Properties of A356 Aluminum Alloy, *Mater. Sci. Eng. A*, 2007, **464**, p 249–254
17. R. Li, R. Li, Y. Zhao, L. He, C. Li, H. Guan, and Z. Hu, Age Hardening Behavior of Cast Al-Si Alloy, *Mater. Lett.*, 2004, **58**, p 2096–2101
18. H. Liao, Y. Sun, and G. Sun, Correlation Between Mechanical Properties and Amount of Dendritic α-Al Phase in As-Cast Near-Eutectic Al–11.6% Si Alloys Modified with Strontium, *Mater. Sci. Eng. A*, 2002, **335**, p 62–65
19. H. Liao, Y. Sun, and G. Sun, Restraining Effect of Strontium on the Crystallization of Mg2Si Phase During Solidification in Al–Si–Mg Casting Alloys and Mechanisms, *Mater. Sci. Eng. A*, 2003, **358**, p 164–170
20. W.F. Miao and D.E. Laughlin, Precipitation Hardening in Aluminum Alloy 6062, *Scripta Mater.*, 1999, **40**, p 873–878
21. S.W. Youn and C.G. Kang, Characterization of Age-Hardening Behavior of Eutectic Region in Squeeze-Cast A356–T5 Alloy Using Nanoindenter and Atomic Force Microscope, *Mater. Sci. Eng. A*, 2006, **425**, p 28–35
22. O. Umezawa and K. Nagai, Microstructural Refinement of an As-Cast Al-12.6wtpct Si Alloy by Repeated Thermo Mechanical Treatment to Produce a Heavily Deformable Material, *Metall. Mater. Trans. A*, 1999, **30**, p 2221–2228
23. K. Ding, Microstructures and Mechanical Properties of Al-Si-Mg Alloys Under Different Heat Treatment Histories, Southeast University, School of Materials Science and Engineering, MSc. Nanjing, 2008
24. Y. Fei, M. Jin, J. Li, and G.J. Shao, Effect of Cold Deformation on Aging Precipitation Process of 6082 Al-Mg-Si Alloy After Solution Treatment, *Heat Treat. Met.*, 2006, **31**, p 68–71
25. M. Ferry and P.R. Munroe, Enhanced Recovery in a Particulate-Reinforced Aluminium Composite, *Mater. Sci. Eng. A*, 2003, **358**, p 142–151
26. M. Cai, D.P. Field, and G.W. Lorimer, A Systematic Comparison of Static and Dynamic Aging of Two Al-Mg-Si Alloys, *Mater. Sci. Eng. A*, 2004, **373**, p 65–71
27. H.J. Roven, M. Liu, and J.C. Werenskiold, Dynamic Precipitation During Severe Plastic Deformation of an Al–Mg–Si Aluminium Alloy, *Mater. Sci. Eng. A*, 2008, **483–484**, p 54–58